

**A New Model for the Formation of Shatter Cones : Consequences for the Interpretation  
of Shatter Cone Data in Terrestrial Impact Structures  
D. Baratoux<sup>1</sup>, H.J. Melosh<sup>2</sup>**

Corresponding author : David Baratoux

<sup>1</sup>Laboratoire Dynamique Terrestre et Planétaire  
14, Avenue Edouard Belin  
31000 Toulouse, France  
Phone : (33) 5 61 33 29 79  
e-mail : david.baratoux@cnes.fr  
<sup>2</sup>Lunar and Planetary Laboratory,  
University of Arizona Tucson, AZ 85721, USA  
Phone: (520) 621-2806  
e-mail : jmelosh@lpl.arizona.edu

Words count : 4884  
Pages count : 11  
8 Tables  
7 Figures

---

**Abstract**

In this paper we present a new model for the formation of shatter cones. The model follows earlier suggestions that shatter cones are initiated by heterogeneities in the rock, but does not require the participation of an elastic precursor wave: the conical fractures are initiated after the passage of the main plastic compression pulse, not before. Numerical simulations using the hydrocode SALE 2D, enhanced by the Grady-Kipp-Melosh fragmentation model, support the model. The conditions required for the formation of shatter cones are explored numerically and are found to be consistent with the pressure range derived from both explosion experiments and the analysis of shock metamorphic features in impact structures. This model permits us to deduce quantitative information about the shape of the shock wave from the shape and size of the observed shatter cones. Indeed, the occurrence of shatter cones is correlated with the ratio between the width of the compressive pulse and the size of the heterogeneity that initiates the conical fracture. The apical angles of the shatter cones are controlled by the shape of the rarefaction wave.

## Introduction

Shatter cones are the characteristic form of rock fractures in impact structures. They have been used for decades as unequivocal fingerprints of meteoritic impact on Earth [1]. The abundant data about shapes, apical angles, sizes and distribution of shatter cones for many terrestrial impact structures may provide insights in the determination of impact conditions and characteristics of shock waves produced by high-velocity projectiles in rocks. However, the mechanism of the formation of shatter cones remains to date enigmatic and a quantitative interpretation of these data is therefore not possible.

Relevant models for the formation of shatter cones must be consistent with the following constraints given by the observations of shatter cones in various high-pressure shocked materials including natural impact structures and explosion experiments. Shatter cones are found over a broad range of sizes of impact structures. They have been reported beneath the floors of small craters such as Kaalijarvi, Estonia (110 m), Lonar, India (1800 m) and Ries, Germany (24 km) [2]. At Charlevoix, shatter cones are well developed about 7 km from the center of the crater, with progressive decrease in quantity inward and outward [2]. The pressures reached during shatter cone formation can be estimated from shock metamorphic features [3]. Shock metamorphic minerals formed by high-pressure shocks (coesite, stishovite, shock-formed glass, planar features) are observed closer to the shock wave source, whereas shatter cones are commonly located further out the shock source area. All these observations imply a restricted range of pressure allowing the formation of shatter cones. The minimum formation pressure appears to be at least 1 GPa [2], while the maximum pressure is usually a few GPa. However, at the Charlevoix structure shatter cones are found at pressures up to about 20 GPa. Shatter cones have also been produced by explosion in various rocks [2,4]. In these experiments shatter cones are also observed within a restricted pressure range that extends from 2 GPa to 6 GPa [2].

The axes of shatter cones are generally described as pointing toward the shock wave source area in both natural impact structures and explosion experiments [1]. However, many cases of non-radial orientations are now known [5]. These occurrences are probably the result of non-spherical propagation of the shock wave due to the complex interaction of shock waves with non-uniform rock targets [6]. The size of natural shatter cones ranges from few centimeters to 12 meters. Parts of cones are more common than a complete conical surface and striations are observed at the surface of fractures. Apical angles are reported to vary from approximately 60° to 120° with an average value close to 90° [1,2,7,8]. The presence of spherules, indicating shock-induced melting, is reported at the Vredefort structure, South Africa [9,10].

Different mechanisms have been proposed to explain the formation of shock-induced conical fractures. The most widely accepted mechanism is based on a theoretical study of the phenomenon by Johnson and Talbot [11]. They proposed that shatter cones form when the elastic precursor of the shock front is scattered by a heterogeneity in the rock. The scattered elastic wave then interacts interferes with the direct wave inside a conical region. The plastic limit inside this conical region is exceeded, while stresses remain below this limit outside the volume. If the stress is removed before the arrival of the plastic wave, the material outside (which returns elastically to its original state) separates along the conical boundary. However, both gage records from underground nuclear tests [12] and numerical simulations [6] show there is never zero-stress interval between the elastic precursor and the main plastic wave.

Material could also relax behind an elastic wave, but it is not clear that such a relaxation produces suitable conditions for the operation of the Johnson-Talbot mechanism [7]. Following these comments, Milton was the first to propose that shatter cones may form during the relaxation after the compression peak rather than before [7]. Recently, Sagy et al. proposed a model to explain the formation of striations [13]. While this model is valuable for the interpretation of the branching microstructures commonly seen on the surfaces of shatter cones, it does not provide an explanation for the conical shapes of these fractures.

## **Mechanism for the formation of shatter cones**

A clear understanding the stress patterns that develop during the expansion of a spherical stress wave is a basic prerequisite to any model of shatter cone formation. Furthermore, because we propose that shatter cones are tensional fractures, it is important to understand when and where tensional stresses develop during the propagation of a shock wave. Before presenting our new model, we thus describe in detail the stresses in an expanding spherical shock wave. Later in the paper we show how these stresses are modified by the presence of a simple heterogeneity.

### **Shock waves in spherical geometry**

Although analytical solutions exist for the propagation of pure elastic waves in spherical geometry, there is no such solution for plastic or shock waves. To evaluate the radial and hoop stresses both at and behind the shock front, we performed a simple 1-dimensional simulation in spherical geometry using the numerical code SPALL [14]. SPALL is a one-dimensional Lagrangian hydrocode [15] that includes the Grady-Kipp-Melosh fragmentation model and uses a nonlinear Murnhagan equation of state [16] and an elastic-plastic yield model [17]. We compute the propagation of a radially compressive stress wave with an initially triangular profile through a grid made of 300 cells. The rise time of the pulse is 0.1 ms and the decay time is 1 ms. The properties of the material are given in table 1. Many different computations with different initial shock waves were performed. All showed qualitatively similar behavior. We report here the detailed results from a computation of the propagation of a plastic wave in a spherical shell whose radius ranges between 80 meters and 120 meters (see figure 1). Both hoop and radial stresses are compressive during the rising portion of the wave and at some distance behind the shock front. An elastic precursor appears when the velocity of the plastic wave becomes slower than the velocity of the sound. This situation occurs when the value of the pressure peak is just above the Hugoniot elastic limit (1GPa in this computation). During the decay of the plastic wave (never in the rising portion), the hoop stress becomes tensional while the radial stress is still compressive. The radial stress becomes slightly tensional at later time, but hoop stress is always the most tensional. This numerical simulation supports the existence of a tensional hoop stress occurring during the decay of the shock wave. We suggest that this hoop stress sets the stage for the tensional formation of shatter cones.

### **Description of the model**

The mechanism we present here relies on the scattering produced by heterogeneities in the rocks. However, our mechanism is different from the one proposed by Johnson and Talbot (1964). Indeed, a tensional stress is required for the formation of shatter cones in our model. Our model relies on the interaction of a scattered elastic wave with the tensional hoop stress

that develops behind the front in spherical geometry (see figure 2). When the shock front encounters a heterogeneity whose material properties imply a lower sound speed (lower bulk modulus or higher density), an extensional wave is generated and propagates radially from the heterogeneity. In the case of high velocity heterogeneity, the scattered wave is compressive, and thus cannot lead to further tensile fracture. As the main shock front propagates away from the site of the heterogeneity, the hoop stress, initially compressive reduces to zero and finally becomes tensional. Consider the total stress at any given time. The tensional hoop stress interferes constructively with the tensional scattered wave. For some critical value of the hoop stress, the interference produces a tensional stress above the tensile resistance of the material. Thus, fracture may occur at the locations indicated by filled-circles on figure 2.

The advance of both the scattered and the main shock waves produces fractures along a conical surface (Actually, the exact shape of the structure is given by the successive intersections of two expanding spheres. This can be approximated by a cone for only a restricted range of distances). One can argue that this tensional stress along the boundary of a cone is the precondition for the formation of striations according to the mechanism proposed by Sagy and Reches (2002). The volume inside the conical surface is mechanically isolated from the surrounding rock mass and is thus preserved from further fracturing. Indeed, the excess of tensional stress along the boundary of the cone localizes the fragmentation to a narrow region.

## Two-Dimensional Numerical model

### Mesh geometry

The Navier Stokes equations are solved in spherical geometry using the 2 dimensional hydrocode SALE 2D. SALE 2D is capable of solving of wide range of problems, from low-velocity fluid flow to hypervelocity shock phenomena [18].

The Lagrangian mesh used in all simulations has the shape of a spherical shell defined by 4 parameters: the internal radius, the external radius, the angle and the radial dimension of the cells (see figure 3). To simulate a continuative boundary for the external surface and avoid any reflection of the direct wave from this boundary, the size of the last 20 cells is progressively increased by a factor of 1.1 for each successive layer.

### The Grady-Kipp-Melosh fragmentation model

When stress becomes tensional our model employs Grady-Kipp-Melosh's dynamic fragmentation model [19,20] implemented in our version of SALE 2D. The Grady-Kipp model treats the accumulation of fracture damage as a continuous process. The effect of each individual fracture is integrated into a scalar parameter called damage,  $D$ , which is responsible for a decrease of the elastic moduli when the material is in tension:

$$\sigma_{ij} = K(1-D)\varepsilon\delta_{ij} + 2\mu(1-D)\left(\varepsilon_{ij} - \frac{1}{3}\varepsilon\delta_{ij}\right) \quad (1)$$

where  $\sigma_{ij}$  is the stress tensor,  $\varepsilon_{ij}$  the strain tensor,  $K$  and  $\mu$  the bulk and shear moduli respectively and  $\varepsilon$  the scalar volume strain equal to  $\varepsilon_{11} + \varepsilon_{22} + \varepsilon_{33}$ .

The damage  $D$  is related to the number and size of cracks in the rocks by the equation:

$$D = nV \quad (2)$$

where  $n$  is the number of idealized penny-shaped cracks per unit volume and  $V$  is the volume of the spherical stress-relieved region surrounding a crack. The damage at any time is an integral over the damage that has accumulated in the history of the material:

$$D(t) = \int_{-\infty}^t \frac{dn}{dt}(t')(t-t')dt' \quad (3)$$

The number of flaws activated at any time is given by two-parameters,  $k$  and  $m$ , through the Weibull distribution [21]:

$$N = k\varepsilon^m \quad (4)$$

where  $N$  is the number of flaws per unit volume activated at or below the tensile strain  $\varepsilon$ . Grady and Kipp (1980) assumed that cracks, once activated, grow at their maximum speed  $c_g$ , from which they derived the fundamental integral equation for damage accumulation:

$$D(t) = \frac{4}{3}\pi c_g^3 \int_{-\infty}^t \frac{dN}{d\varepsilon}(1-D)(t-t')^3 dt' \quad (5)$$

One of the interesting characteristics of this damage model is that the failure stress depends upon strain rate: higher strain rates imply higher yield stresses.

In the Weibull model, a threshold strain must exist for the initiation of damage accumulation. The size of this threshold is inversely controlled by the size of the fragmenting body [22]. Indeed, for an infinite body, a flaw can always be found that fails for any small arbitrary strain. However, for a finite body of radius  $R$ , the activation of at least one flaw at a given small strain implies that the failure strain is greater than:

$$\varepsilon_{\min} = \left(\frac{4}{3}\pi k R^3\right)^{-1/m} \quad (6)$$

In the numerical simulations, we use a size-dependant minimum strain at which cracks can initiate. The reader is referred to the complete description of the numerical implementation of this model in [22].

### Numerical stability

A shock wave is usually treated as a discontinuity in state variables [16] and must satisfy the Rankine-Hugoniot jump conditions. However, the numerical treatment of shock waves requires additional forces for the purposes of computational stability. Stability can not be insured by usual methods when such a discontinuity is present [23]. SALE 2D is capable of solving a wide range of problems, from low-velocity fluids flow to hypervelocity shock phenomena with the help of artificial viscosity and coupling between adjacent nodes [18]. We use a value for the coefficient ARTVIS equal to 1.0 within SALE 2D for modeling the propagation of stress waves, since this was the lowest value that consistently maintains wave stability behind the front shock.

The effects of the artificial viscosity are negligible when shocks are not present. We have checked that the artificial viscosity does not affect the velocity and stress across the

smear-out jump, which accordingly obey the Hugoniot equations. To insure numerical stability it has been also found necessary to use a physical viscosity. The use of a physical viscosity is supported by the explosion experiments in rock, reported in [20]. Values of 10 MPa-s are used in our simulations, as suggested by this study. This parameter does not affect the Rankine-Hugoniot conditions, but does have some effect on the rise time of the shock wave.

The fragmentation model implies an additional cost of computation, because damage accumulation in a failing cell is generally the fastest physical process. The time step is chosen to limit the damage increase in each cell to 3% per iteration as in [22].

## **Results**

### **Stresses scattering by a heterogeneity**

This section and the simulation presented here are intended to illustrate the interaction between the tensional hoop stress and the scattered wave that we propose to be responsible for the formation of shatter cones. This preliminary simulation does not use any fragmentation model and the Hugoniot elastic limit is above the stresses everywhere in the mesh and at any time. Thus, plastic deformation does not occur. Consequently, this computation is only intended to understand the propagation of elastic waves in the vicinity of a heterogeneity in the rock, which gives support to our model.

In this simulation, the dimension of the mesh is 150 \* 100 cells, the angle of the cone is 30°, the radial size of the cells is 2 cm and the internal radius of the shell is 7 m. The heterogeneity is defined by a region of 2 cells \* 2 cells. The top boundary of the heterogeneity, toward the center of the spherical shell, is located at the 30th cell, which corresponds to a distance of 7.60 m from the source. The parameters of the materials are detailed in Table 2. The pressure input pulse is 1 GPa, its rise time is 0.01 ms and its decay time is 0.1 ms.

The maximum stress (tension is positive) at different stages of the computation is reported here (see figure 4). The elastic wave scattered by the heterogeneity extends in all directions at the velocity of the sound in the material, producing a spherical extensional wave centered on the heterogeneity. As demonstrated in the 1-dimensional simulations in spherical geometry, the hoop stress becomes tensional behind the shock front. The tensional hoop stress and the scattered wave interfere constructively. Thus, if the minimum stress or strain is exceeded where the intersection occurs (arrows on figure 4), damage is expected to accumulate along the boundary of a conical region.

### **Conditions for the formation of shatter cones**

Although the modification of the stress pattern by the presence of a heterogeneity is qualitatively relevant to the formation of shatter cones, numerical simulations are required to investigate the exact conditions for such fractures. Indeed, once damage has accumulated for one cell, tensional stress is no longer transmitted by this cell, leading to a highly non-linear process. Thus, we investigate here the conditions suitable for shatter cones to form. The relevant parameters that might affect the formation of shatter cones include material properties (density, bulk and shear moduli, Hugoniot elastic limit) as well as the shape and magnitude of the stress wave. The next step, which is beyond of the scope of this paper, is the

quantitative relation of the detailed shapes of shatter cones (sizes, apical angles) to the impact conditions.

In the simulations reported in this section, the angle of the spherical shell is again  $30^\circ$  and the left boundary of the heterogeneity (toward the center of the spherical shell) is also located at the 30th cell, corresponding to a distance of 7.60 m to the center of the spherical shell whose internal radius is 7 meters. For example, when a region of 2 cells \* 2 cells defines the area where a heterogeneity occurs, the corresponding dimensions are 4 cm \* 7.2 cm. The pulse has a triangular shape in all simulations and is defined by its maximum pressure, its rise time and the decay time factor ( $\beta$ ), which is the ratio of the decay time to the rise time. The Hugoniot elastic limit is held at 50 GPa for these simulations, so that no plastic deformation occurs. The influence of the plastic yielding will be addressed later.

### **Sound velocity of materials**

We first investigated the properties required for a heterogeneity that produces a scattered wave strong enough to allow damage accumulation. In these simulations, the maximum pressure in the input pulse is 3 GPa, the rise time is 0.01 ms and the decay time factor 0.05. We will discuss later the relevance of these parameters to the real world. The simulations were performed with a fixed density and 4 different bulk modulus ratios between the surrounding rock and the heterogeneity of: 100, 10, 5 and 2 (the shear modulus is modified to hold the Poisson's ratio constant). Since the sound velocity scales as the root square of these moduli, the velocity ratio ranges from 10 to  $\sqrt{2}$ . All others parameters are held constant. We display the history of the stress and damage for the simulation with the velocity ratio equal to  $\sqrt{10}$  (see figure 5). The stress and damage history demonstrates that the model we propose can operate with these initial conditions. A cone is formed at the end of the simulation whose size is about 1 meter at its base, and its apical angle is close to  $90^\circ$ .

From these simulations, it appears that a shatter cone develops for a velocity ratio greater or equal to 2.2. Other simulations are required with both different values of density and bulk modulus to define more precisely those physical properties of the material and the heterogeneity that allow our mechanism to work. However, such velocity ratios are commonly seen in geological media as seen in [24] who reports data in the range of 1.5 km/s to 7.8 km/s. Our mechanism is thus likely to occur in many different geologic media.

### **Influence of the peak pressure**

Next, we investigate the influence of the maximum pressure, as many authors report that shatter cones are only observed for a restricted range of pressure. The pulse shape is identical to the previous computation and the bulk modulus ratio is set to 10 (bulk modulus is 50 GPa and shear Modulus is 30 GPa in the surrounding rock). This average value corresponds to a velocity ratio common in geologic media. All parameters except pressure peak are held constant. The pressure peak is given as the input value of the pressure at the left boundary. However, there is a small decrease of the pressure through our grid due to wave divergence in the spherical geometry, but we neglect this small decay in the formation conditions reported here.

For low pressures, below 2 GPa in our simulations, damage accumulates only in a restricted area at the edge of the heterogeneity and does not extend to other parts of the material. From 3 GPa to 6 GPa, shatter cones develop. However, for the highest pressure, partial damage begins to accumulate even inside the cones. At pressures above 7 GPa, damage is equal to one almost everywhere at the end of the computation. We interpret the upper limit for the pressure as follows: the ratio between the magnitude of the tensional stress resulting from the constructive interference and the hoop stress that occurs everywhere in the grid decreases at higher pressure. Consequently, the tensional hoop is not relieved fast enough along the boundary of the cone and thus accumulates more uniformly in the grid. The rock is crushed everywhere, but tensile failure does not concentrate along the surface of a cone.

The range of pressure suitable for the formation of shatter cones resulting from these simulations is strikingly similar to the range of pressure observed in natural shatter cones or shatter cones formed in explosive experiments. This result thus strongly supports the model proposed in this paper. The range of pressure observed for shatter cones therefore seems to be controlled by the dynamic resistance of the material in tension, and not by the Hugoniot limit as previously thought.

### **Influence of the rise time**

Finally, we investigated the influence of the rise time of the pulse compared to the size of the heterogeneity, or the corresponding time for the wave to travel across the heterogeneity. We report in all the following simulations the size of the heterogeneity along the radial direction (or along the propagation direction of the stress wave), see table 5. Larger cells (20 cm instead of 2 cm) were used for the second set of the simulations, and the radius of the shell were also multiplied by a factor 10.

The occurrence of shatter cones seems to be highly correlated with the ratio between the rise time and the size of the heterogeneity. However, the rise time of a shock wave produced by high-velocity impact in geologic media is unknown, since it has been never measured. It is often assumed that the rise time is of the order of  $L/v$  where  $L$  is an equivalent radius of the projectile and  $v$  the velocity [16]. Adopting a reasonable ratio between the velocity of the projectile and the sound velocity in the target, the width of the pulse is a fraction of the size of the projectile. However, applying such a rationale, to most impact structures where shatter cones are observed, does not yield results consistent with the idea that shatter cones are produced by a centimeter or millimeter-scale heterogeneity in the rock. Furthermore, our simulations demonstrate that shatter cones occur only when the ratio between the pulse width and the size of the heterogeneity is close to 1. To date, no good theoretical treatment of the shape of the shock wave is available. However, some experimental data have been acquired for shock waves from explosions [20] and laboratory impacts on metal targets [25]. These observations demonstrate, first, that the rise time and the shape of the shock is a characteristic of the material and not a characteristic of the source of the wave. Second, few relationships have been established experimentally between the rise time and the particle velocity. Consider, for example, the relationship derived from one of these experiments [20] for salt material:

$$\tau = 0.038v_{\max}^{-0.6} \quad (7)$$

where  $\tau$  is the rise time and  $v_{\max}$  the maximum velocity of the particle. Using the Hugoniot equation and the material parameters used in our simulation, we derive:

$$\tau = 0.0038 \left( \frac{P}{\rho U} \right)^{-0.6} = 90 * P^{-0.6} \quad (8)$$

This experimental relationship has been validated for low-pressure shocks (in the range of 10 MPa to 100 MPa). If we extrapolate this relation to a shock pressure of 3 GPa, we find a rise time of 0.1 ms still larger (by a factor 10) than the rise times we used in our computations. However, the non-linear increase of the velocity for high pressure may produce a thinner shock for stress waves of several GPa than that estimated by equation (8) above. Moreover, the presence of shatter cones at the scale of centimeters may indicate that the rise time of a stress wave produced by an impact is smaller than previously thought. On the other hand, if the widths of shock waves are as large as a few meters in geologic media, the hypothesis of an interaction between a direct wave and a scattered wave can not be valid. In summary, the rise time of strong shock waves in geologic media is an important, but presently unclear issue in our comprehension of impact processes.

### **Example of formation of a shatter cone in a basaltic target**

We present an example of a numerical simulation of a shatter cone formation (see figure 6), based on the hypothesis that an inclusion of ice is present in a basaltic material. Since we have explored the various ranges of conditions suitable for the formation of shatter cones with fictitious materials, we demonstrate here that the mechanism also operates in this particular and natural example. We used a mesh of 150\*100 cells with an internal radius of 7 meters. The radial size of the cells is 0.02 m. The angle of the spherical shell is 30°. The parameters of the two materials are given in Tables 6 and 7. The Hugoniot limits of basalt and ice are poorly known, and we use very approximate values of respectively 1 and 0.1 GPa according to common ranges of values reported for a number of rocks [16]. The parameters of the stress wave are given in Table 8.

### **Some consequences for the analysis of shatter cone data**

Our proposed mechanism for the formation of shatter cones only operates if the width of the shock wave is comparable to the dimensions of the heterogeneity, which also must be smaller than the shatter cone. The pulse width of the shock consequently must be thinner than previously thought. Moreover, the size and distribution of shatter cones provides a critical constraint on the shape of the shock wave.

Apical angles of shatter cones vary from 60° to 120°. These simulations do not yet fully define all of the parameters that influence the apical angle of the cones. One of the main factors must be the decay time, which has a direct influence on the delay between the passage of the shock front and the arrival of the tensional hoop stress.

A simple geometric model highlights the factors relevant to the determination of the apical angles in shatter cones. Consider, as a first order approximation, that the delay between the shock wave and the tensional hoop stress is equal to the decay time of the stress wave  $\beta\tau$ , where  $\tau$  is the rise time. If the radius of the direct shock wave is large, the front can be approximated by a plane, at least for small distances compared to the radius, and the angle of the shatter cone is (see figure 7):

$$\theta(t) = 2 * \arccos\left(1 - \frac{\beta\tau}{\delta t}\right) \quad (9)$$

where  $\delta t$  is the time elapsed since the contact between the shock front and the heterogeneity. The reported angles of shatter cones (60° to 120°) correspond to values of  $\delta t/\tau$  that range from 2 to  $2/\sqrt{3}$ . These values are consistent with the time at which the damage accumulates in our simulations.

In conclusion, this formula indicates, first, that the apparent apical angle observed on a part of a shatter cone depends on the decay time of the shock wave. Second, this approximate formula illustrates also the influence of the parameters of the heterogeneity: the magnitude of the extensional and spherical scattered wave decreases during its propagation and the maximum time  $\delta t$  during which this wave is strong enough to initiate damage only along the boundary of the conical region depends on the properties of the heterogeneity, in particular the sound velocity ratio between the heterogeneity and the surrounding material. The influence of all these factors must be explored further by means of numerical simulations to interpret the apical angle data of shatter cones and their likely variations as a function of distance to the source (e.g. as reported in [13]).

## Conclusion

A new model for the formation of shatter cones has been investigated by means of numerical simulations. The mechanism proposed here operates over a wide range of conditions and for materials with properties similar to common geologic media. However, the mechanism operates only within a restricted range of pressures, 3 GPa to 6 GPa, which is strikingly close to the range of pressures derived from both observations of natural shatter cones and shatter cones produced by explosion experiments. The model gives results consistent with the reported apical angles and the observation that cones commonly point toward the source (deviations from this relationship may be due to scattering and consequent non-radial propagation of the main shock wave). The size and distribution of shatter cones in impact structures appear to be correlated with the ratio between the size of the heterogeneity and the pulse width of the shock wave. From this result, the rise time of shock wave in geological media is shorter than previously believed, otherwise this mechanism can not operate. According to this model, the apical angle depends on both the properties of the heterogeneity and the decay time of the shock wave. None of these simulations, except the inclusion of ice in basalt, include a significant amount of plastic deformation. The Hugoniot elastic limits of rocks vary considerably even among rocks of the same type, and thus the effect of plastic deformation during the fragmentation invites further study.

## Acknowledgments

This work was performed during a visit of the first author to the Lunar and Planetary Laboratory, University of Arizona. It was supported by NASA Grant NAG5-11493 and a post-doctoral fellowship from CNES.

## References

- [1] R.S. Dietz, Meteorite Impact suggested by shatter cones in rock, *Science*, 131, (1960), 1781-1784.

- [2] D.J. Roddy, L.K. Davis, Shatter cones formed in large-scale experimental explosion craters, in: D.J. Roddy, R.O. Pepin, R.B. Merrill, (Ed.), *Impact and Explosion Cratering*, Pergamon Press, New York, USA, (1977), pp. 715-750.
- [3] B.M. French, *Traces of Catastrophe: A handbook of shock-metamorphic effects in terrestrial meteorite impact structures*, LPI Contribution No. 954, Lunar and Planetary Institute, Houston TX, (1998), 120 pp.
- [4] E. Schneider, G.A. Wagner, Shatter cones produced experimentally by impacts in limestone targets, *Earth Planet. Sci. Lett.*, 203, (1976), 40-44.
- [5] L.O. Nicolaysen, W.U. Reimold, Vredefort shatter cones revisited, *J. Geophys. Res.*, 104, (1999), 4911-4930.
- [6] D.E. Grady, Processes occurring in shock wave compression of rocks and minerals, in: M. H. Manghanani and S.-I. Akimoto (Ed.), *High-Pressure Research: Applications in Geophysics*, Academic Press, New York, USA, (1977), pp 389-438.
- [7] D.J. Milton, Shatter cones - An outstanding problem in shock mechanics, in: D.J. Roddy, R.O. Pepin, and R.B. Merrill (Ed.), *Impact and Explosion Cratering: New York*, Pergamon Press, (1977), 703-714.
- [8] R.M. Stesky, H.C. Halls, Structural analysis of shatter cones from the state Islands, northern Lake superior, *Canadian Journal of Earth Sciences*, 20, (1983), 1-18.
- [9] N.L. Gay, Spherules on shatter cones surfaces from the Vredefort structure, *South Africa, Science*, 194, (1972), 724.
- [10] H.M. Gibson, Shock-induced melting and vaporization of shatter cones surfaces: Evidence from the Sudbury impact structure, *Meteoritics and Planetary Science*, 33, (1998), 329-336.
- [11] G. Johnson, R. Talbot, A theoretical study of the shock wave origin of shatter cones. M.s. Thesis, Air Force Int. Tech, Wright-Patterson AFB, Ohio, USA. (1969), 170 pp.
- [12] W.R. Perret, R. C. Bass, Free-Field ground motion induced by underground explosions, SAND74-0252, Sandia National Lab (1975).
- [13] A. Sagy, Z. Reches, J. Fineberg, Shatter-cones: Dynamic fractures generated by meteoritic impacts, *Nature*, 418, (2002), 310-313.
- [14] H.J. Melosh, H.J., High-velocity solid ejecta fragments from hypervelocity impacts, *Intern. Journ. of Impact Eng.*, 5, (1987) 483-492.
- [15] R.D. Richtmyer, K. W. Morton, in: *Interscience (Ed), Difference methods for initial-value problems*, (1967).
- [16] H.J. Melosh, *Impact cratering, A geologic Process*, Oxford University Press, New York, USA, (1989), 245 pp.
- [17] Anderson, C. E., An overview of the theory of hydrocodes, *Int. J. Impact Eng.*, 5, (1987), 33-59.
- [18] A. Amsden, H. M. Ruppel and C. W. Hirt, SALE: A Simplified ALE Computer Program for Fluid Flow at All Speeds, LA-8095, Los Alamos National Laboratory (1980).
- [19] D.E. Grady, D.E., M.E. Kipp, Continuum modeling of explosive failure in oil shale, *Int. J. R. Mech. Min. Sci. Geomech. Abstr.*, 17, (1980), 147-157.
- [20] H.J. Melosh, H.J., Shock viscosity of explosion waves in geologic media, submitted to *J. Appl. Phys.*
- [21] J.C. Jaeger, *Elasticity, Fracture and Flow*, Methuen (Ed), London (1969).
- [22] H.J. Melosh, E.V. Ryan, Dynamic fragmentation in impacts: Hydrocode simulation of laboratory impact, *Journ. of Geophys. Res.*, 97, (1992), 14735-14759.
- [23] J. VonNeumann, R. D. Richtmyer, A method for the numerical calculation of hydrodynamic shocks, *J. Appl. Phys.* 21, (1950), 232-237.

- [24] F. Birch, Compressibility; Elastic constants, in: S. P. Clark (Ed.), Handbook of Physical Constants, GSA Memoir 97, Geol. Soc. Amer., New York, USA, (1966), pp. 107-173.
- [25] J.W. Swegle, and D. E. Grady, Shock viscosity and the prediction of shock wave arrival times, *J. Appl. Phys.* 58, (1985), 603-701.

Density kg/m <sup>3</sup>	Bulk Modulus (GPa)	Shear Modulus (GPa)	Murnhagan Exponent	Hugoniot Elastic limit (GPa)
3000	50	30	4	1

Table 1. Material properties in the 1-dimensional simulation of the propagation of a spherical shock wave.

	Material	Heterogeneity
Density (kg/m <sup>3</sup> )	3000	3000
Bulk Modulus (GPa)	50	5
Shear Modulus (GPa)	30	3
Murnhagan Exponent	4	4
Hugoniot Elastic Limit (GPa)	50	50

Table 2. Material parameters.

Bulk Modulus of Heterogeneity(GPa)	0.5	5.0	10.0	25.0
Bulk Modulus Ratio	100	10	5	2
Velocity Ratio	10	3.2	2.2	1.4
Shatter cone	Yes	Yes	Yes	No

Table 3. Influence of the bulk modulus and the velocity ratio between the material and the heterogeneity.

Pressure (GPa)	1	2	3	4	6	7
Shatter cone	No	No	Yes	Yes	Yes	No

Table 4. Influence of the maximum pressure of the shock wave.

Size of the heterogeneity(m)	0.04	0.04	0.04	0.08	0.08	0.08	0.16	0.16	0.16
Rise time of the stress wave (ms)	0.01	0.02	0.04	0.01	0.02	0.04	0.01	0.02	0.04
$\beta$ (decay time factor)	5	5	5	5	5	5	5	5	5
Ratio rise/time/inh. time	1.37	2.73	5.47	0.68	1.37	2.73	0.34	0.68	1.37
Shatter cone	Yes	Yes	No	Yes	Yes	No	Yes	Yes	Yes

Size of the heterogeneity (m)	0.4	0.4	0.4	0.8	0.8	0.8	1.6	1.6	1.6
Rise time of the stress wave (ms)	0.01	0.02	0.04	0.01	0.02	0.04	0.01	0.02	0.04
$\beta$ (decay time factor)	5	5	5	5	5	5	5	5	5
Ratio rise/time/inh. time	1.37	2.73	5.47	0.68	1.37	2.73	0.34	0.68	1.37
Shatter cone	Yes	Yes	No	Yes	Yes	No	Yes	Yes	Yes

Table 5. Influence of the rise time and the size of the heterogeneity.

Density	Bulk Mod.	Shear Mod.	Murnhagan	$c_g$	pweib	cweib
---------	-----------	------------	-----------	-------	-------	-------

kg/m <sup>3</sup>	GPa	GPa	exponent	m/s	m	m <sup>-3</sup>
2980	60.1	36.7	5.5	1790	9.05	3.05*10 <sup>40</sup>

*Table 6. Parameters of the material (Basalt) (Melosh, 1992).*

Density kg/m <sup>3</sup>	Bulk Mod. GPa	Shear Mod. GPa	Murnhagan exponent	c <sub>g</sub> m/s	pweib m	cweib m <sup>-3</sup>
900	0.2	0.12	5.23	7500	8.7	3.2*10 <sup>44</sup>

*Table 7. Parameters of the heterogeneity (Ice) [16,22].*

Pressure (GPa)	Rise time (ms)	Decay time factor
3	0.01	5

*Table 8. Parameters of the stress wave.*

Figure 1. The propagation of a compressive shock wave in spherical geometry derived from our numerical simulations. From top to bottom: velocity of the particle versus distance from the source, radial stress versus distance, and hoop stress versus distance (compression is negative). The elastic precursor is indicated by two arrows on the velocity graph. The hoop stress becomes tensional behind the shock. We suggest that this is the appropriate stress condition for the damage accumulation that leads to the formation of shatter cones.

Figure 2. Schematic representation of our model for the formation of shatter cones. Tensile fracture occurs at the intersection between the scattered tensile wave and the tensile hoop stresses in the main shock wave. When a critical value for the tensional stress is reached, the rock fractures in tension. The fractures accumulate on the surface of a conical region (indicated on the figure by filled-circles and arrows).

Figure 3. Example of the spherical shell used in our simulations. The grid is defined by the following parameters: internal radius, external radius, angle and radial dimension of the cells. Larger cells are used for the larger radii to prolong the grid, thus simulating a continuative outflow boundary and to avoid any reflection of stress waves from this boundary. For those cells, the size ratio of one cell to the next is 1.1.

Figure 4. The propagation of the stress wave at 0.12 ms, 0.17 ms, 0.22 ms and 0.27 ms. Each plot represents the value of the maximum stress, compression is negative, zero stress is represented by the gray level seen, for example, in the still unaffected part of the wave, before the arrival of the shock front responsible for the most negative values. The arrows indicate the position of the extensional scattered wave. The interference between the scattered wave and the tensional hoop stress produces an increased tensional stress along the boundary of a conical region (see the text for further details of the model).

Figure 5. A. Stress history: Time at which the tensional stress exceeds the (average) minimum stress required for damage accumulation (see equation 8). This plot illustrates how the stress responsible for the fragmentation propagates along the boundary of a cone as described in the text. B. Time at which complete damage occurs. The duration of the computation is 0.75 ms. Damage accumulates when the tensional stress is greater than the minimum stress. The relief of the hoop stress as cells are fragmented limits further damage accumulation inside the cone (white cells have damage equal to 0). The two plots are not exactly identical since the maximum stress, which depends on the size of cells, varies along the radius of the spherical shell

Figure 6. Damage history. The duration of the computation is 0.70 ms. The fragmented region expands for the cells along the boundary of the cone, and the hoop stress is consequently relieved after damage occurs. The cells inside the cone remain intact (white cells are not damaged at any time) or only partially damaged.

Figure 7. Simple geometric model for the estimation of the apical angle of the shatter cone.

Figure 1

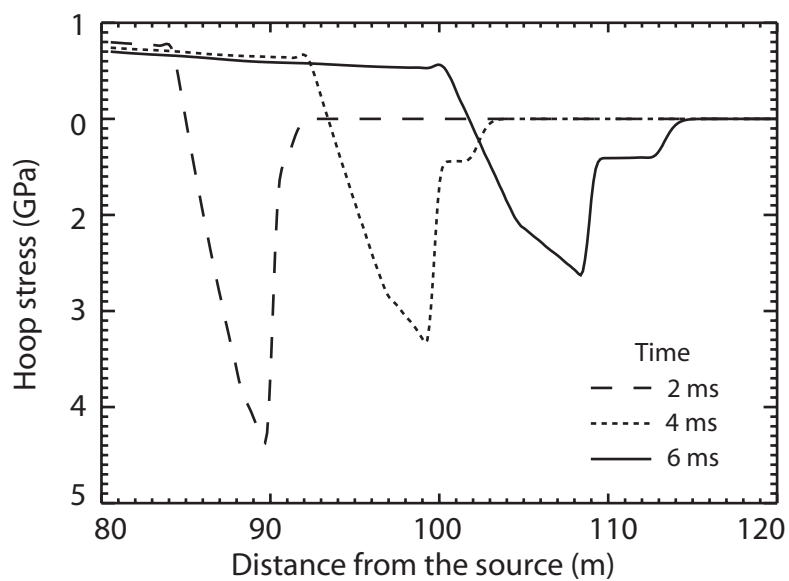
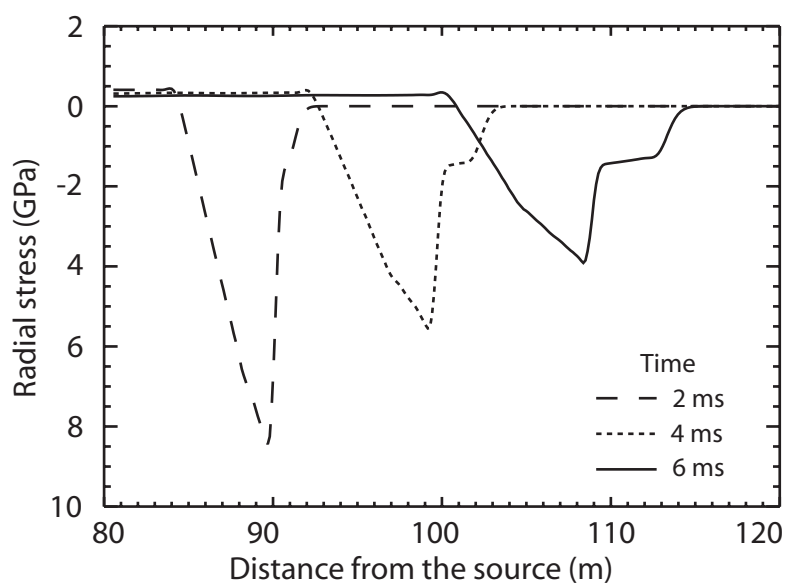
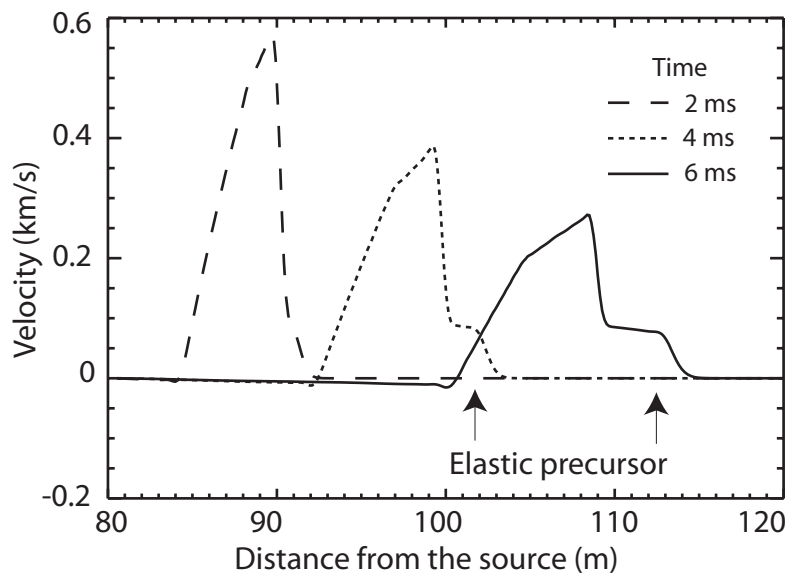


Figure 2

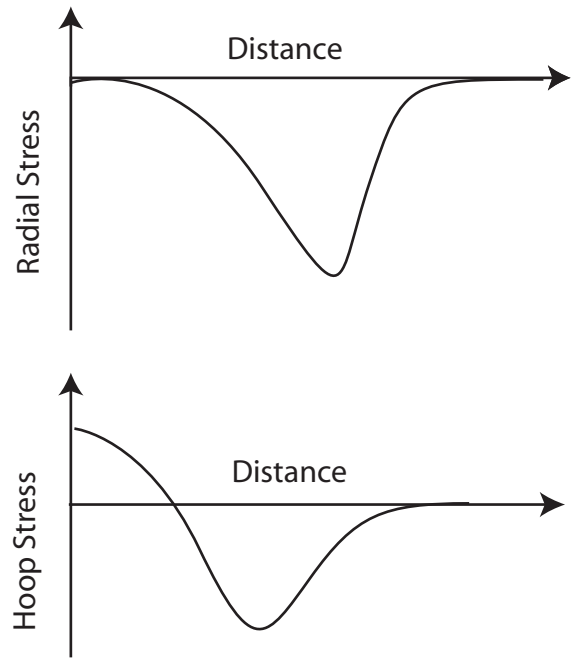
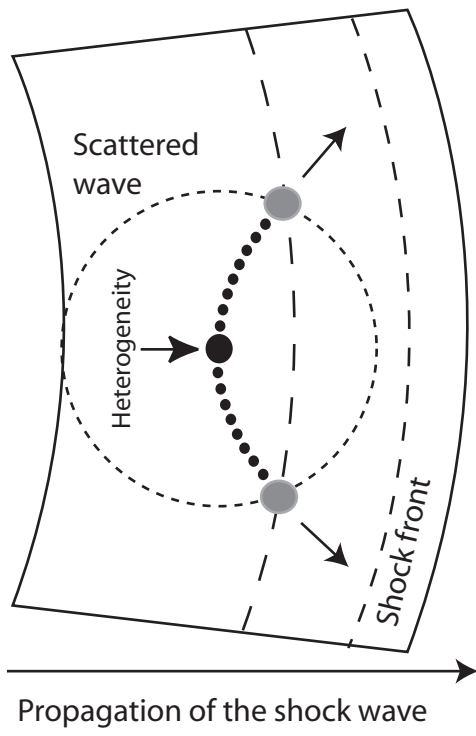


Figure 3

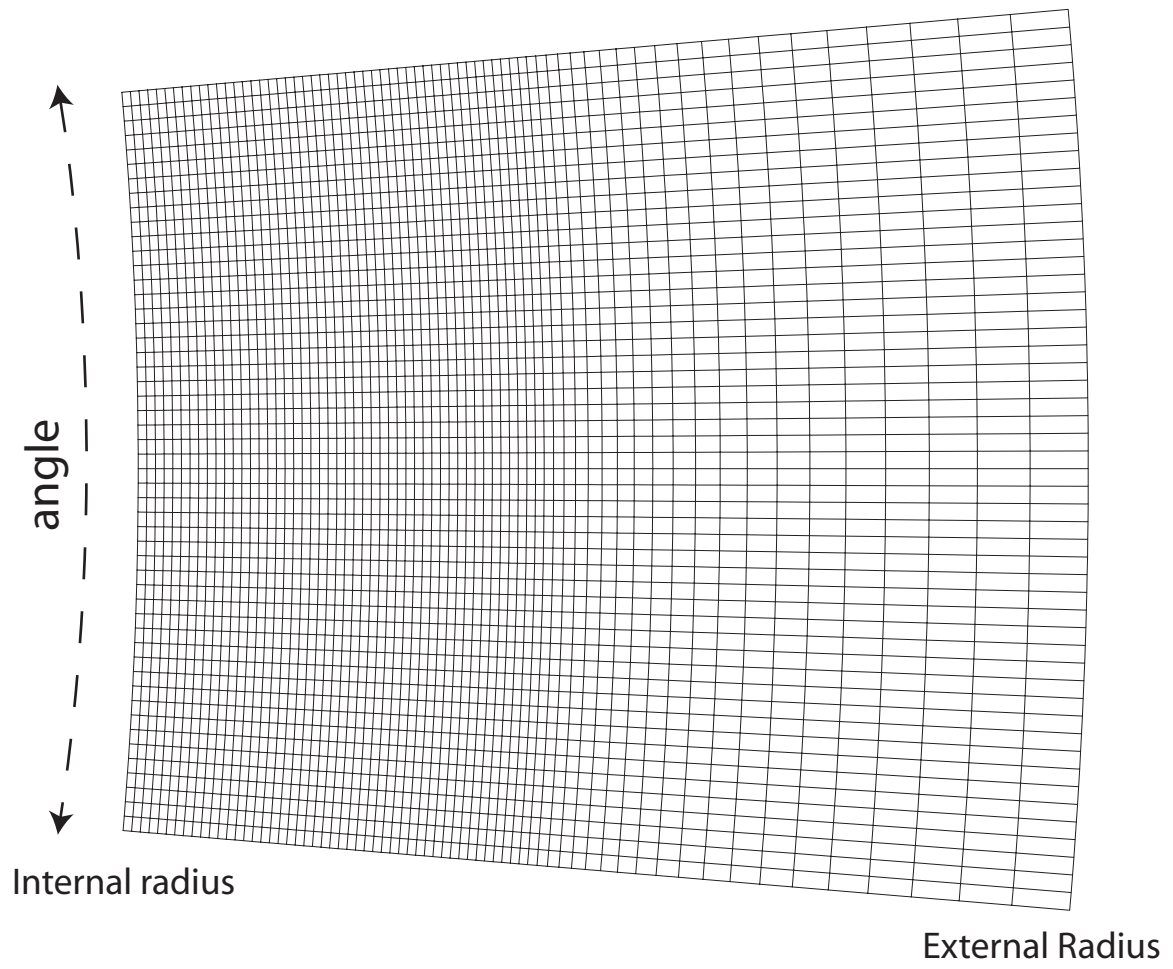
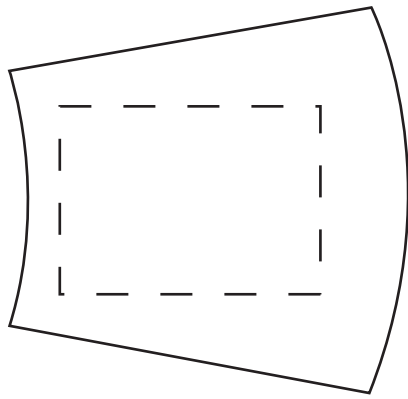
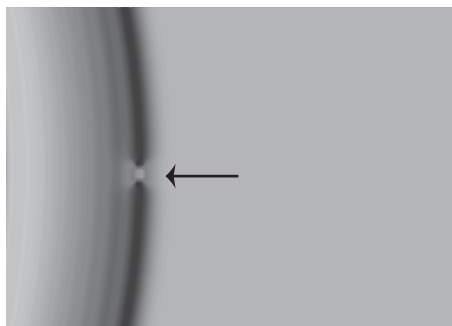


Figure 4



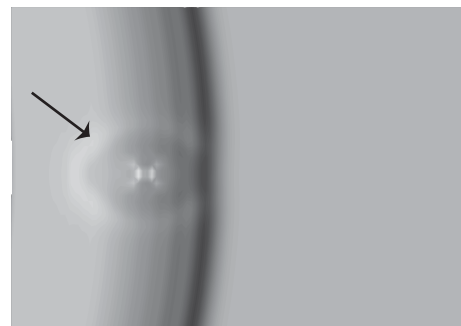
—— Boundary of the shell  
in the computation

- - - Limits of the area  
where the stress is detailed



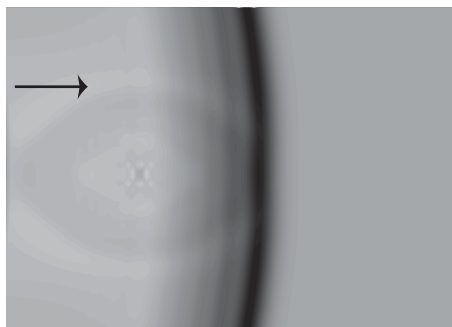
time = 0.12 ms

- 0.35 GPa      0.12 GPa



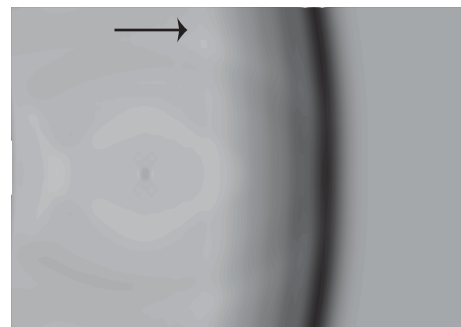
time = 0.17 ms

- 0.3 GPa      0.12 GPa



time = 0.22 ms

- 0.28 GPa      0.12 GPa

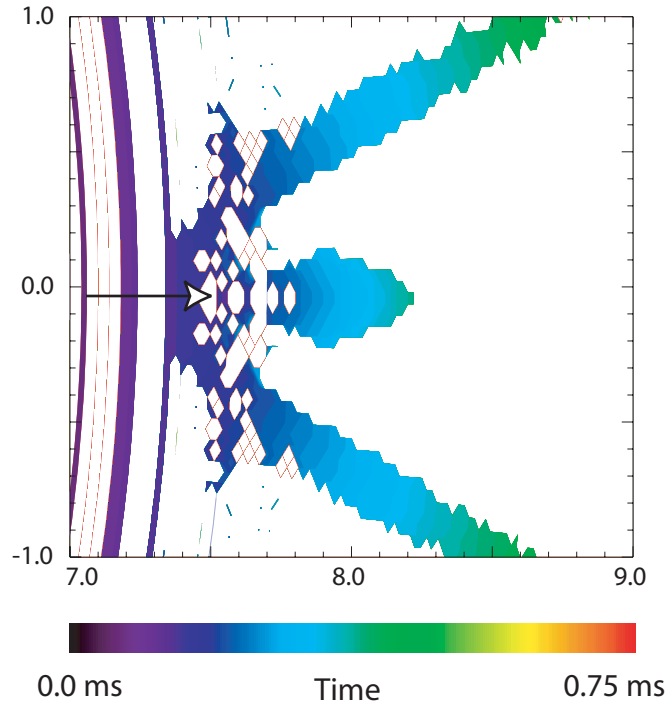


time = 0.27 ms

- 0.28 GPa      0.12 GPa

Figure 5

A. Stress > 65 MPa



B. Damage history

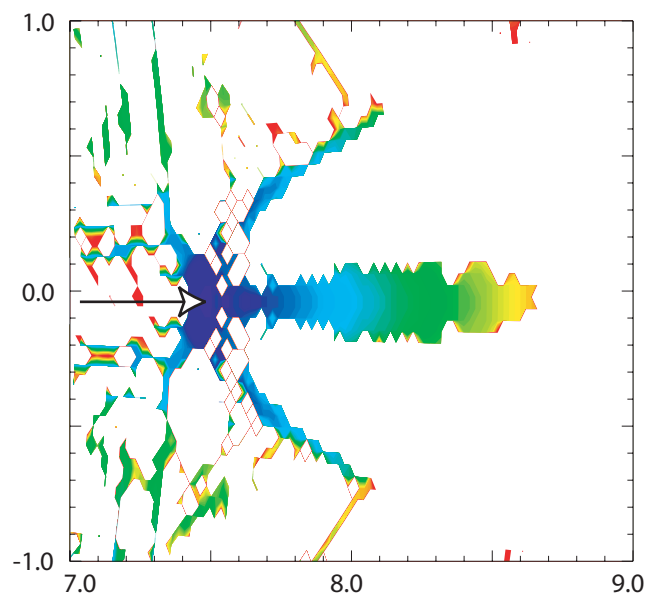


Figure 6

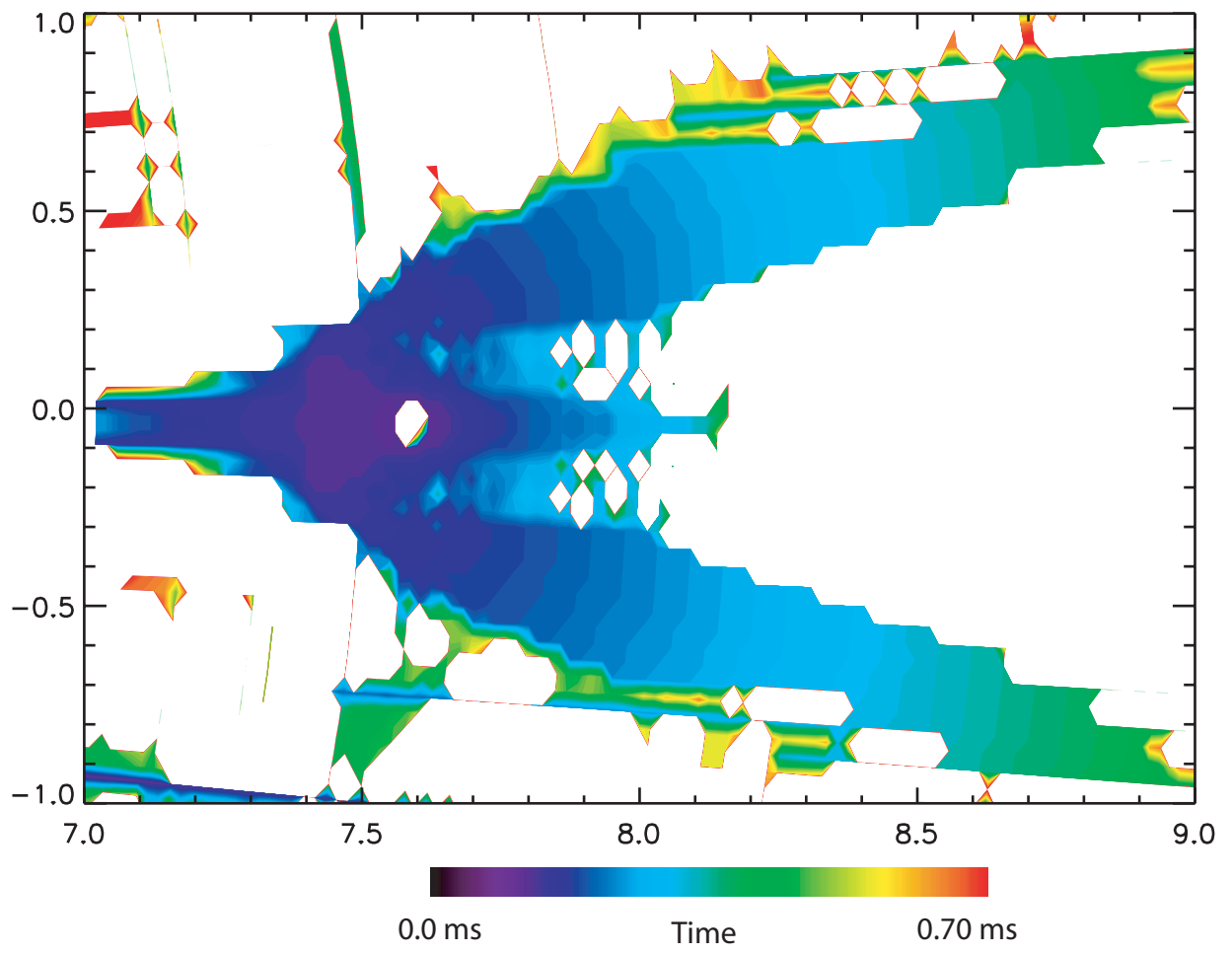


Figure 7

